1. Spectrum of the (single particle) Hamiltonian

(i) PBC: $H = \sum_j \left(\Psi_j^\dagger h_t \Psi_{j+1} + h.c. + \Psi_j^\dagger h_{on} \Psi_j \right)$

periodic boundaries

$\Psi_j^\dagger = (c_{j,A}^\dagger, c_{j,B}^\dagger)$

with $h_t = w \begin{pmatrix} 0 & 0 \\ 1 & 0 \end{pmatrix} = \frac{w}{2}(\sigma_x - i\sigma_y)$

$h_{on} = h \begin{pmatrix} 0 & 1 \\ 1 & 0 \end{pmatrix} = h\sigma_x$

A.2

$\rightsquigarrow \underset{\text{F.T.}}{H} = \sum_k c_k^\dagger \left(h_t e^{ik} + h_t^\dagger e^{-ik} + h_{on} \right) c_k =$ Plug in h_t, h_{on}

$= \sum_k c_k^\dagger \underbrace{\left[(h + w\cos k)\sigma_x + w\sin k\, \sigma_y \right]}_{=: h_k \text{ (Bloch Hamiltonian)}} c_k$

$$h_k = \vec{d}(k) \cdot \vec{\sigma} \quad \text{with} \quad \vec{d}(k) = \begin{pmatrix} h + w\cos k \\ w \sin k \\ 0 \end{pmatrix}.$$

$$E_\pm(k) = \pm |\vec{d}(k)| = \pm \sqrt{(h + w\cos k)^2 + w^2 \sin^2 k}.$$

$$\boxed{(\vec{d}\cdot\vec{\sigma})^2 = |\vec{d}|^2 \cdot \mathbb{1}}$$

⇝ Gapped band structure for $|w| \neq |h|$

⇝ Critical point at $|w| = |h|$.

From now on: $h = 1$, $w \geq 0$, i.e. critical point $w = 1.0$.

(ii) OBC in real space representation:

$$H = \Psi^\dagger h_{rs} \Psi$$

$(c^\dagger_{1,A}, c^\dagger_{1,B}, c^\dagger_{2,A}, \dots, c^\dagger_{L,B})$

with

$$h_{rs} = \begin{pmatrix} (h_{on}) & (h_t) & & \\ (h_t^\dagger) & (h_{on}) & \ddots & \\ & \ddots & \ddots & (h_t) \\ & & (h_t^\dagger) & (h_{on}) \end{pmatrix}$$

Plug in h_{on}, h_t

$$= \begin{pmatrix} 0 & h & 0 & 0 & & & & \\ h & 0 & w & 0 & & & & \\ 0 & w & 0 & h & 0 & 0 & & \\ 0 & 0 & h & 0 & w & 0 & & \\ & & 0 & w & \ddots & & \ddots & \\ & & 0 & 0 & & \ddots & & \\ & & & & \ddots & & 0 & h \\ & & & & & & h & 0 \end{pmatrix}.$$

$\rightsquigarrow$ Fully diagonalize h_{rs} to get all eigenvalues and eigenvectors.

- Spectra (ordered from smallest to biggest eigenvalue) similar with PBC and OBC for $w = 0.5$ (gapped) and $w = 1.0$ (gapless)

- Two extra states at $E \approx 0$ for OBC at $w=2.0$ (as compared to PBC) are localized exponentially at the ends of the lattice

- To see this, plot the modulus of the eigenstates around $E=0$ as a function of j (unit cell index)
- Analytical intuition from fully dimerized limit $\frac{h}{w} \to 0$, e.g. $h=0$, $w=1.0$.

Invariant subspace with 0 energy

$$h_{rs} = \begin{pmatrix} (0) & 0 & 0 & 0 & & \\ 0 & 0 & w & 0 & & \\ 0 & w & 0 & 0 & & \\ 0 & 0 & 0 & 0 & w & \\ & & & w & 0 & \ddots \\ & & & & \ddots & (0) \end{pmatrix}$$

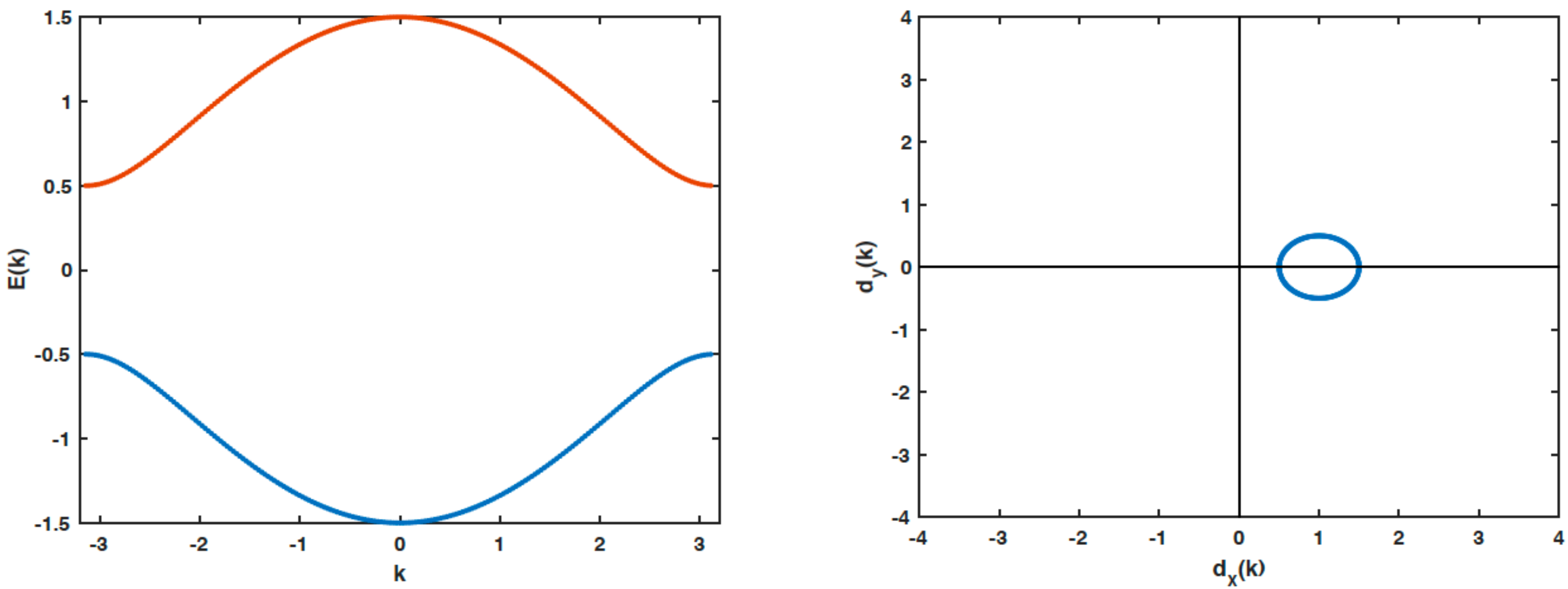

Figure 1: Left panel: Band structure of the SSH model with $h = 1$ and $w = 0.5$. Right panel: Path traced by the $\mathbf{d}(k)$ Bloch vector in the xy plane, for $h = 1$ and $w = 0.5$. Here $L = 200$.

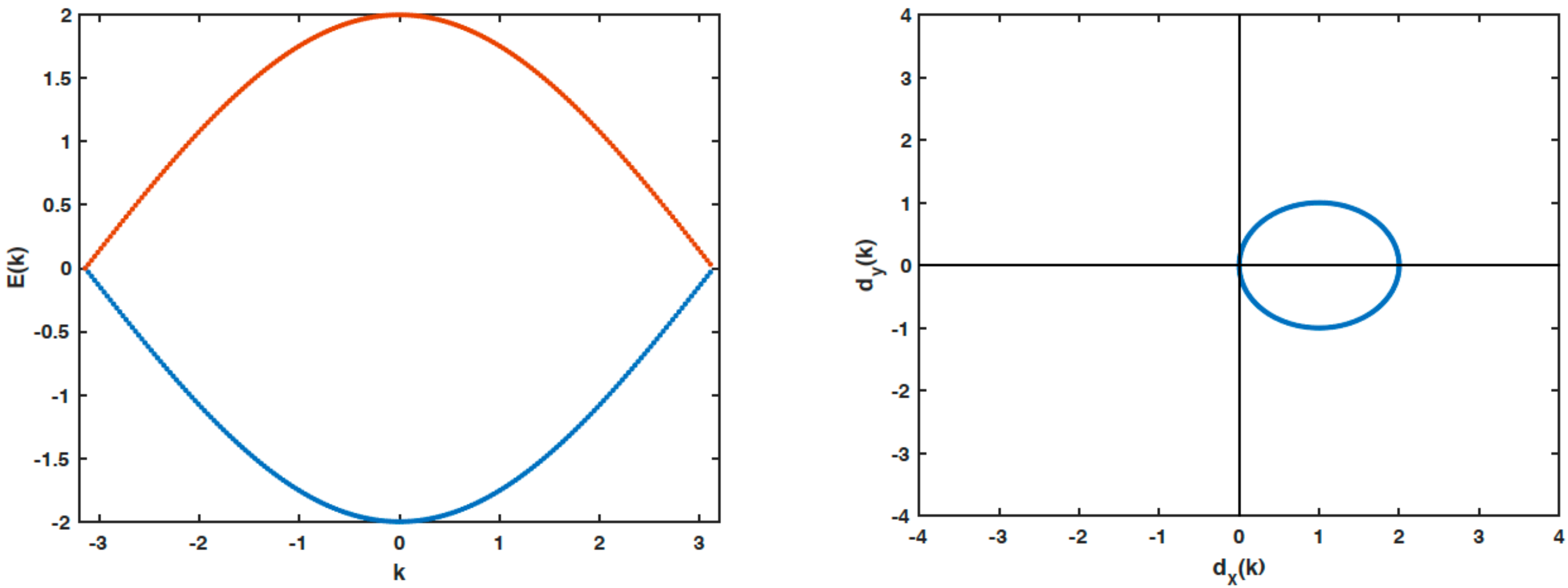

Figure 2: Left panel: Band structure of the SSH model with $h = 1$ and $w = 1$. Right panel: Path traced by the $\mathbf{d}(k)$ Bloch vector in the xy plane, for $h = 1$ and $w = 1$. Here $L = 200$.

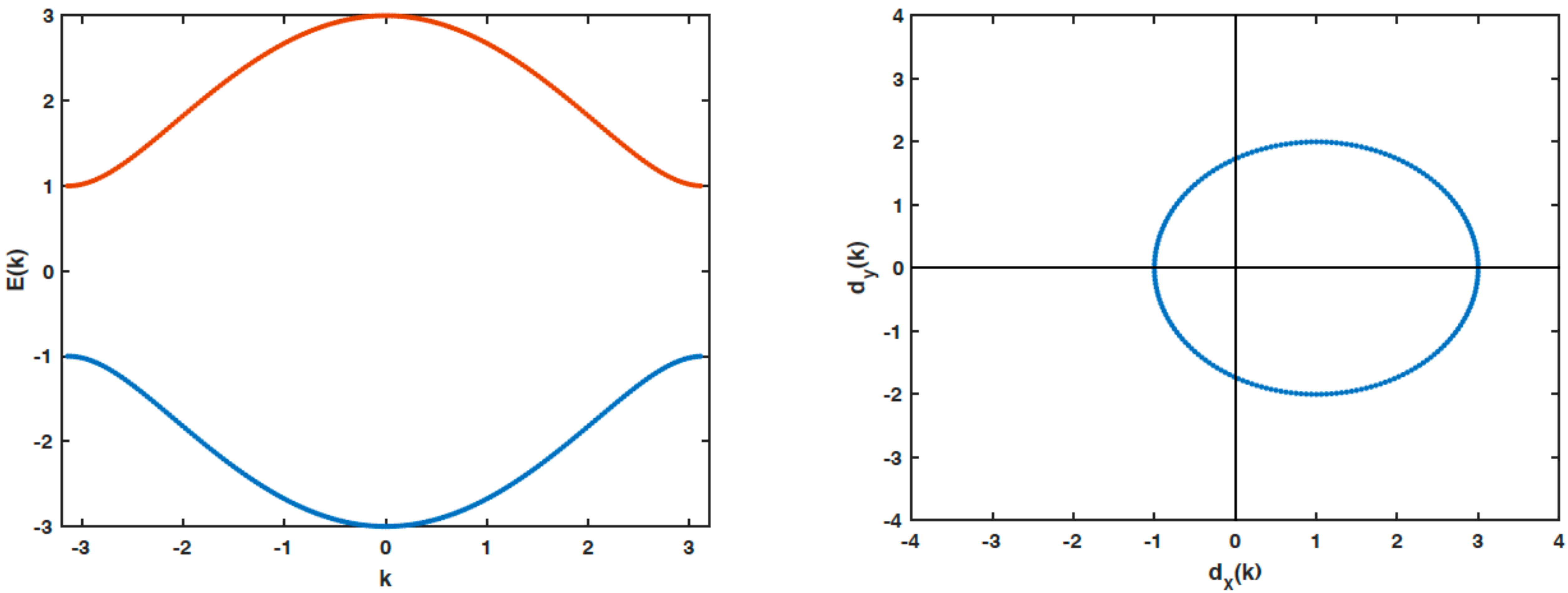

Figure 3: Left panel: Band structure of the SSH model with $h = 1$ and $w = 2$. Right panel: Path traced by the $\mathbf{d}(k)$ Bloch vector in the xy plane, for $h = 1$ and $w = 2$. Here $L = 200$.

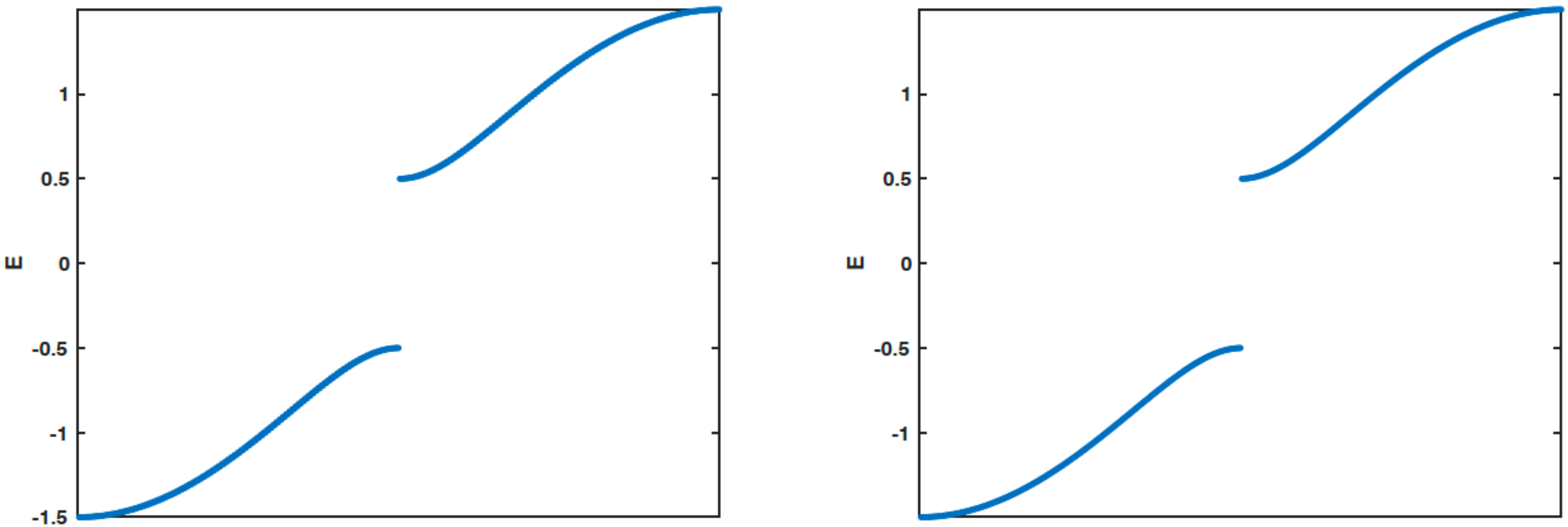

Figure 4: Left panel: Spectrum of the SSH Hamiltonian with PBC and $h = 1$, $w = 0.5$. *Right panel: Spectrum with open boundary conditions, for* $h = 1$, $w = 0.5$. *Here* $L = 200$.

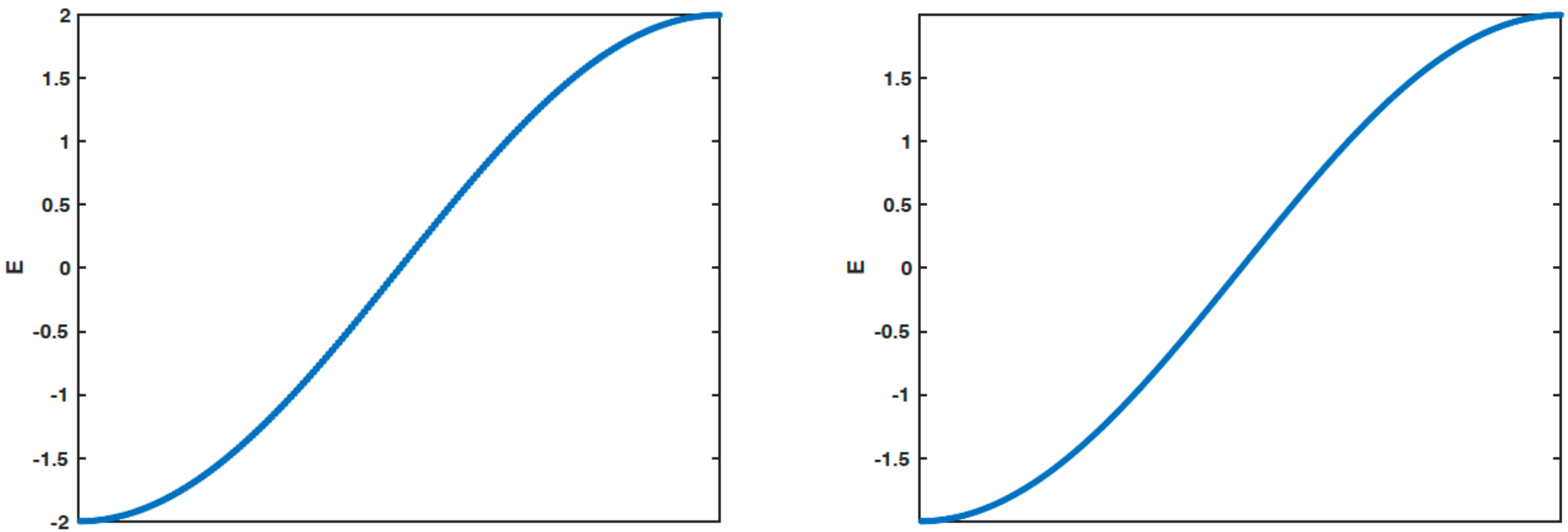

Figure 5: Left panel: Spectrum of the SSH Hamiltonian with PBC and $h = 1$, $w = 1$. *Right panel: Spectrum with open boundary conditions, for* $h = 1$, $w = 1$. *Here* $L = 200$.

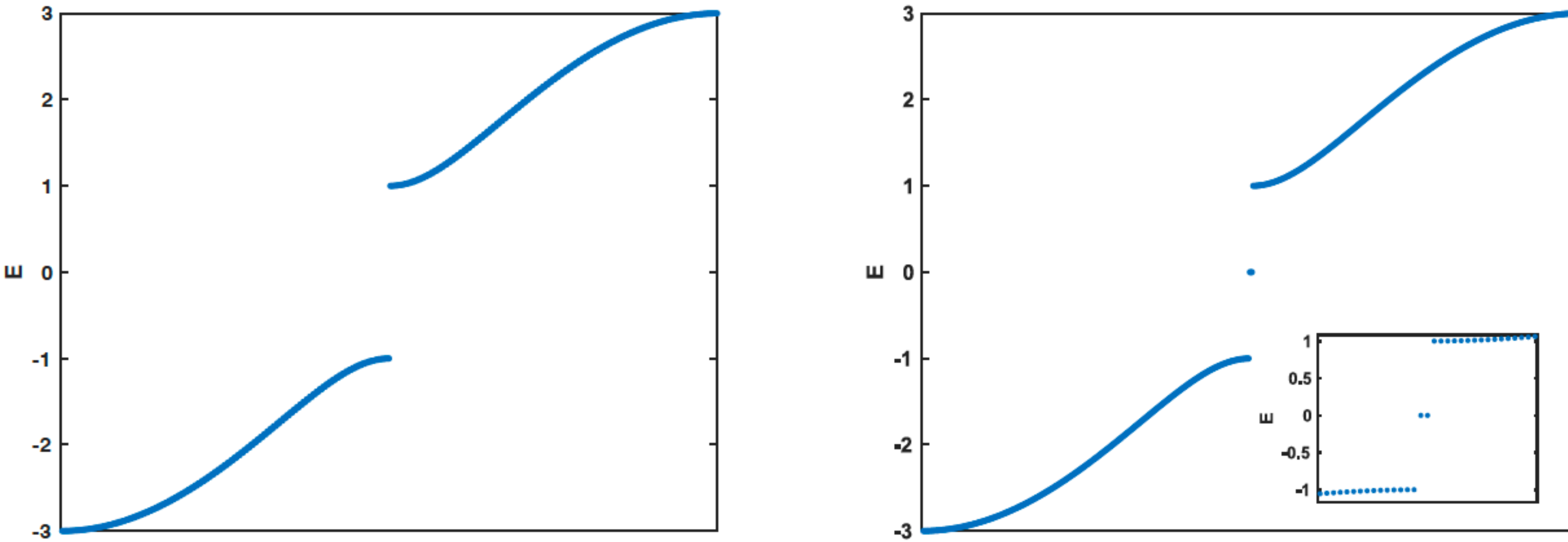

Figure 6: Left panel: Spectrum of the SSH Hamiltonian with PBC and $h = 1$, $w = 2$. Right panel: Spectrum with open boundary conditions, for $h = 1$, $w = 2$, the inset shows in detail the two energy eigenvalues at 0 energy. Here $L = 200$.

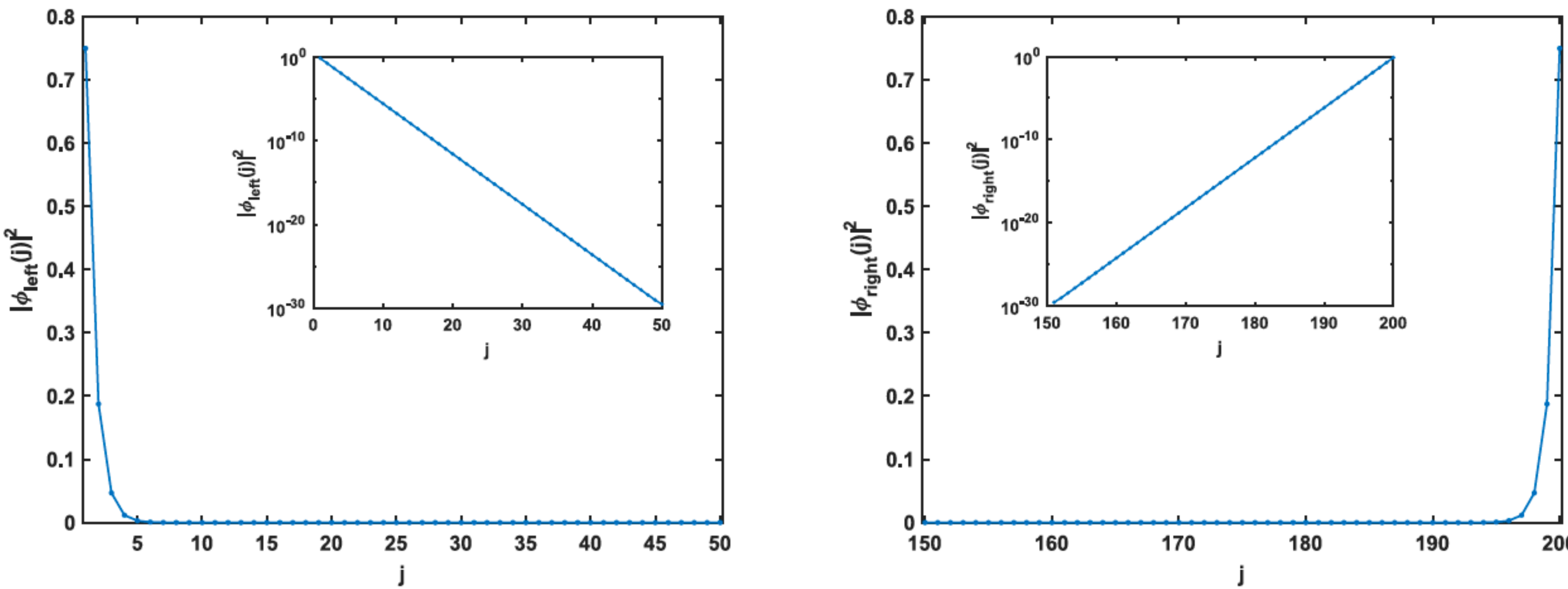

Figure 7: Modulus squared of zero-energy single-particle state wavefunction for $h = 1$, $w = 2$ and $L = 200$. Left panel: State exponentially localized on left end of the SSH chain. Right panel: State exponentially localized on right end of the SSH chain.

$\rightsquigarrow$ Exact eigenstates $|0_L\rangle = \begin{pmatrix} 1 \\ 0 \\ 0 \\ 0 \\ \vdots \\ 0 \end{pmatrix}$; $|0_R\rangle = \begin{pmatrix} 0 \\ 0 \\ \vdots \\ 0 \\ 1 \end{pmatrix}$

satisfy $h_{rs}|0_L\rangle = h_{rs}|0_R\rangle = 0$.

Visualization of dimerization

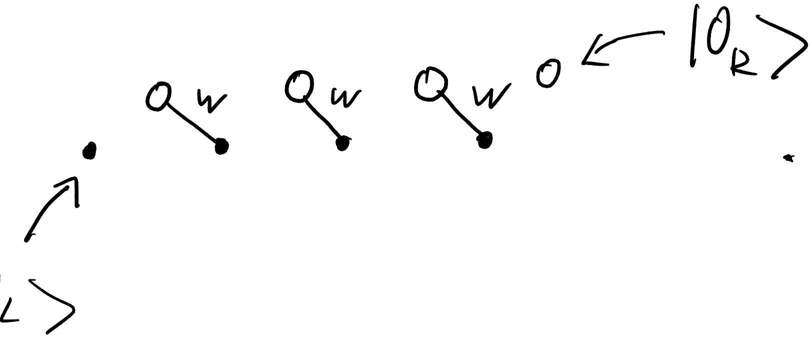

2. Ground state correlation functions at half-filling.

- In full diagonalization of h_{rs}, sort eigenvalues $E_1, \dots, E_{2L}$ from lesser to greater. $|\varphi_1\rangle, \dots, |\varphi_{2L}\rangle$ denote the corresponding eigenstates.

$\rightsquigarrow$ GS at half-filling is a Slater determinant of $|\varphi_1\rangle, \dots, |\varphi_{L=N_f}\rangle$

(no need to calculate anti-symmetrized state explicitly).

Fermions

$N_f = L$

- $G_{A,B}(j,l) = \langle \Psi_0 | \underbrace{c^\dagger_{j,A} c_{l,B}}_{} | \Psi_0 \rangle = \sum_{\alpha=1}^{N_f} \langle \varphi_\alpha | j, A \rangle \langle l, B | \varphi_\alpha \rangle$

$\widetilde{=} \; |j,A\rangle\langle l,B|$

2nd → 1st Q.

boxed formula in A.3

$$= \sum_{\alpha=1}^{N_f} \varphi^*_\alpha(j,A)\, \varphi_\alpha(l,B)$$

position $2l+1$ in eigenvector $\vec{\varphi}_\alpha$ of h_{rs}

position $2j$ (for $j = 0, \dots, L-1$)

↳ We observe exponential decay of G_{AB} with $|j-l|$ for $w = 0.5h$, $w = 2.0h$, and a power-law decay for $w = 1.0\,h$ (critical behavior) $G_{AB} \sim \frac{1}{|j-l|}$.

- Density-density correlations:

Wick

$$\langle \Psi_0 | n_{j,A}\, n_{l,B} | \Psi_0 \rangle - \langle \Psi_0 | n_{j,A} | \Psi_0 \rangle \langle \Psi_0 | n_{l,B} | \Psi_0 \rangle =$$

$$\left[= \langle \Psi_0 | c^\dagger_{j,A}\, c_{j,A}\, c^\dagger_{l,B}\, c_{l,B} | \Psi_0 \rangle \right] = - \langle \Psi_0 | c^\dagger_{j,A}\, c_{l,B} | \Psi_0 \rangle \langle \Psi_0 | c^\dagger_{l,B}\, c_{j,A} | \Psi_0 \rangle$$

Fermi

$$= - G_{AB}(j,l)\, G_{BA}(l,j),$$ and similar combinations for all other combinations of sublattices:

$\hookrightarrow C_{n,n}(j,l) = \langle \Psi_0 | \underbrace{n_j}_{= n_{j,A} + n_{j,B}} n_l | \Psi_0 \rangle - \langle \Psi_0 | n_j | \Psi_0 \rangle \langle \Psi_0 | n_l | \Psi_0 \rangle =$

$$= - G_{A,A}(j,l)\, G_{A,A}(l,j) - G_{B,B}(j,l)\, G_{B,B}(l,j)$$

$$- G_{A,B}(j,l)\, G_{B,A}(l,j) - G_{B,A}(j,l)\, G_{A,B}(l,j).$$

$\rightsquigarrow$ Fit $C_{n,n}(j,l) \sim \dfrac{e^{-\frac{|l-j|}{\xi}}}{|l-j|^{\alpha}}$. We observe that

ξ diverges at critical point $h = w$.

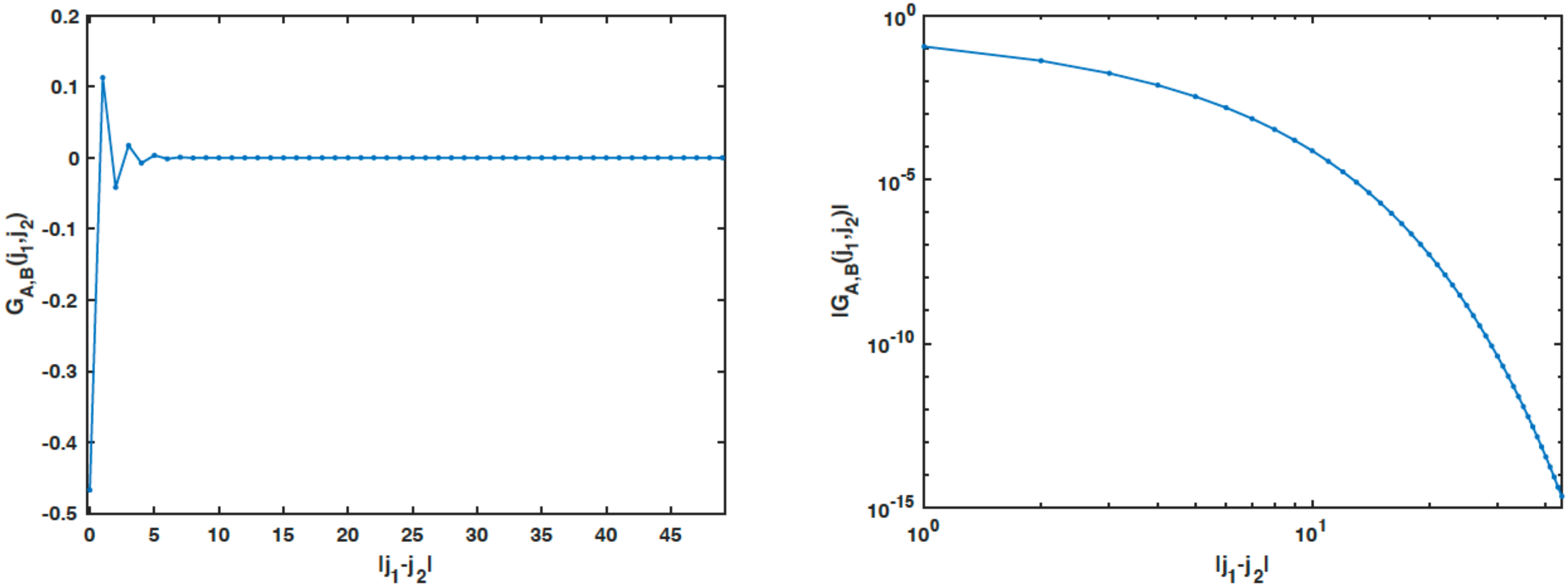

Figure 8: Two-point function $G_{A,B}(j_1, j_2)$ *for* $h = 1$, $w = 0.5$ *with* $L = 200$, $N_{part} = 200$ *and* $j_1 = L/4$, $j_2 \in [L/4, 3L/4]$. *Right panel:* $|G_{A,B}(j_1, j_2)|$ *in log-log scale, showing exponential decay typical of gapped phases.*

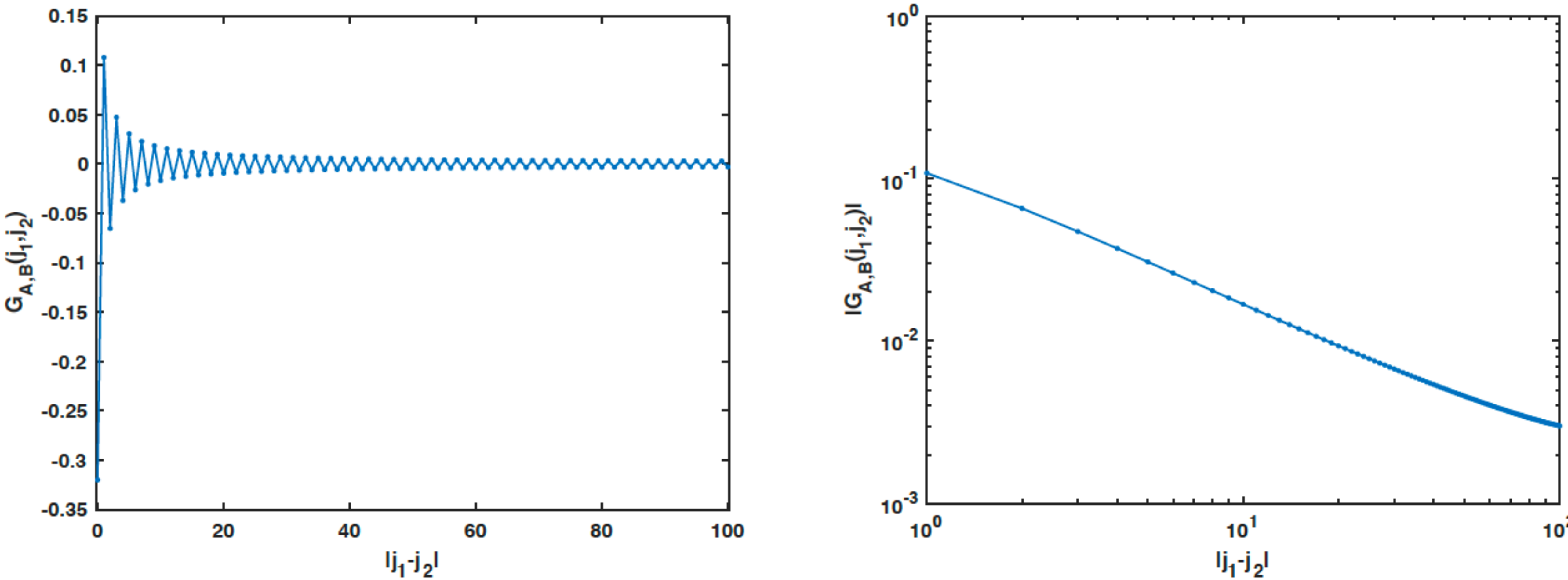

Figure 9: Two-point function $G_{A,B}(j_1, j_2)$ for $h = 1$, $w = 1.0$ with $L = 200$, $N_{part} = 200$ and $j_1 = L/4$, $j_2 \in [L/4, 3L/4]$. Right panel: $|G_{A,B}(j_1, j_2)|$ log-log scale, the decay is power-law at the phase transition.

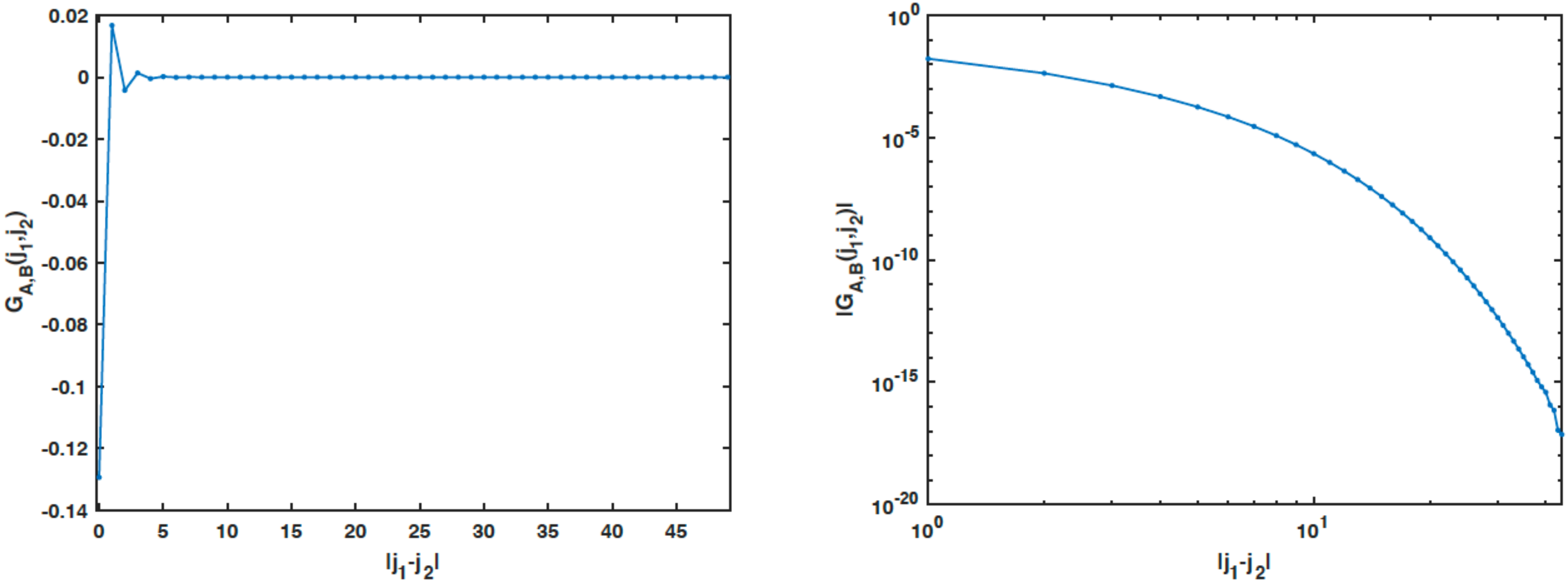

Figure 10: Two-point function $G_{A,B}(j_1, j_2)$ *for* $h = 1$, $w = 2.0$ *with* $L = 200$, $N_{part} = 200$ *and* $j_1 = L/4$, $j_2 \in [L/4, 3L/4]$. *Right panel:* $|G_{A,B}(j_1, j_2)|$ *in log-log scale, showing exponential decay typical of gapped phases.*

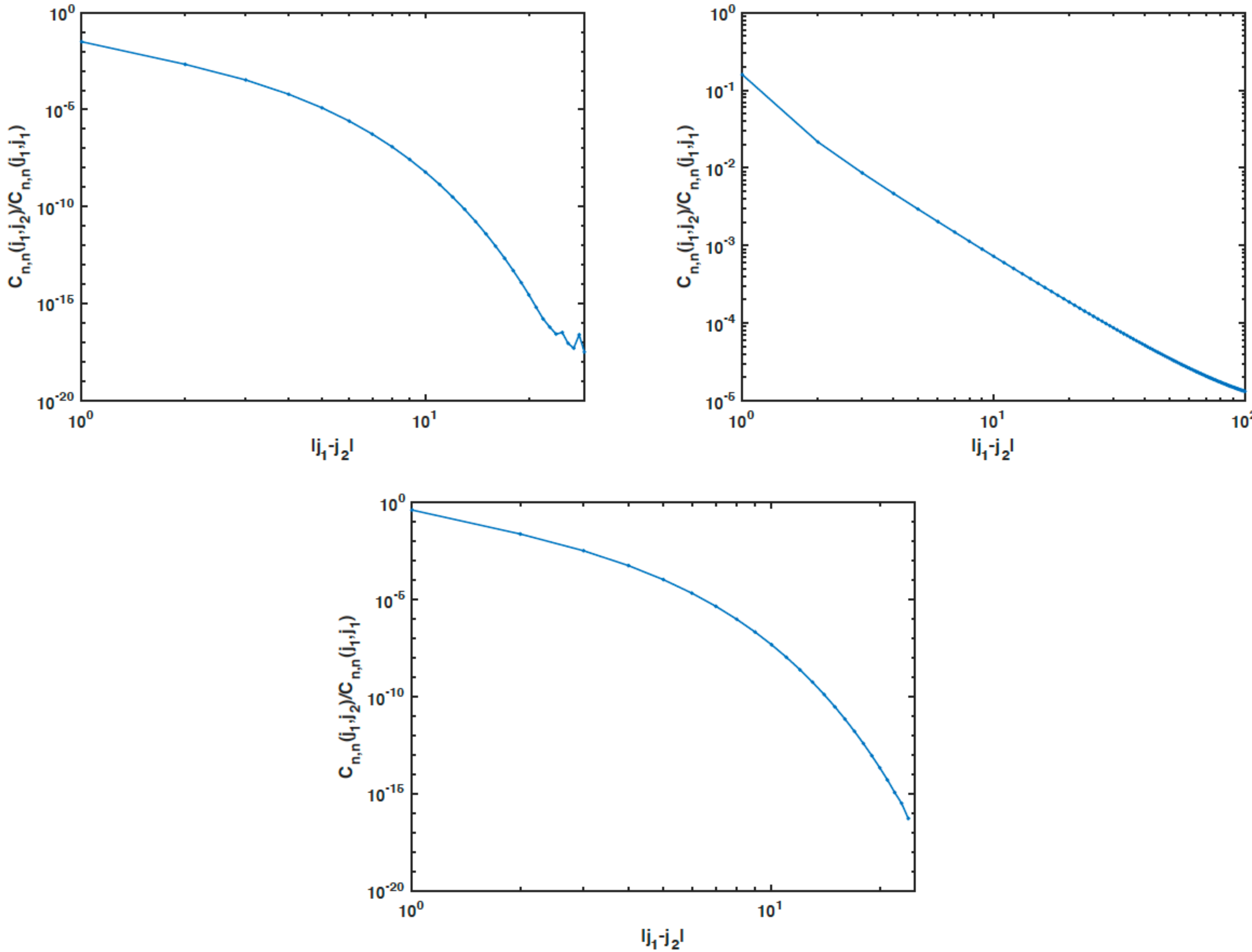

Figure 11: Log-log plots of $C_{n,n}(j_1,j_2)/C_{n,n}(j_1,j_1)$ with $L = 200$, $N_{part} = 200$ and $j_1 = L/4$, $j_2 \in [L/4, 3L/4]$. Upper row, left: $w = 1.5$. Upper row, right: $w = 1.0$. Lower panel: $w = 2.0$.

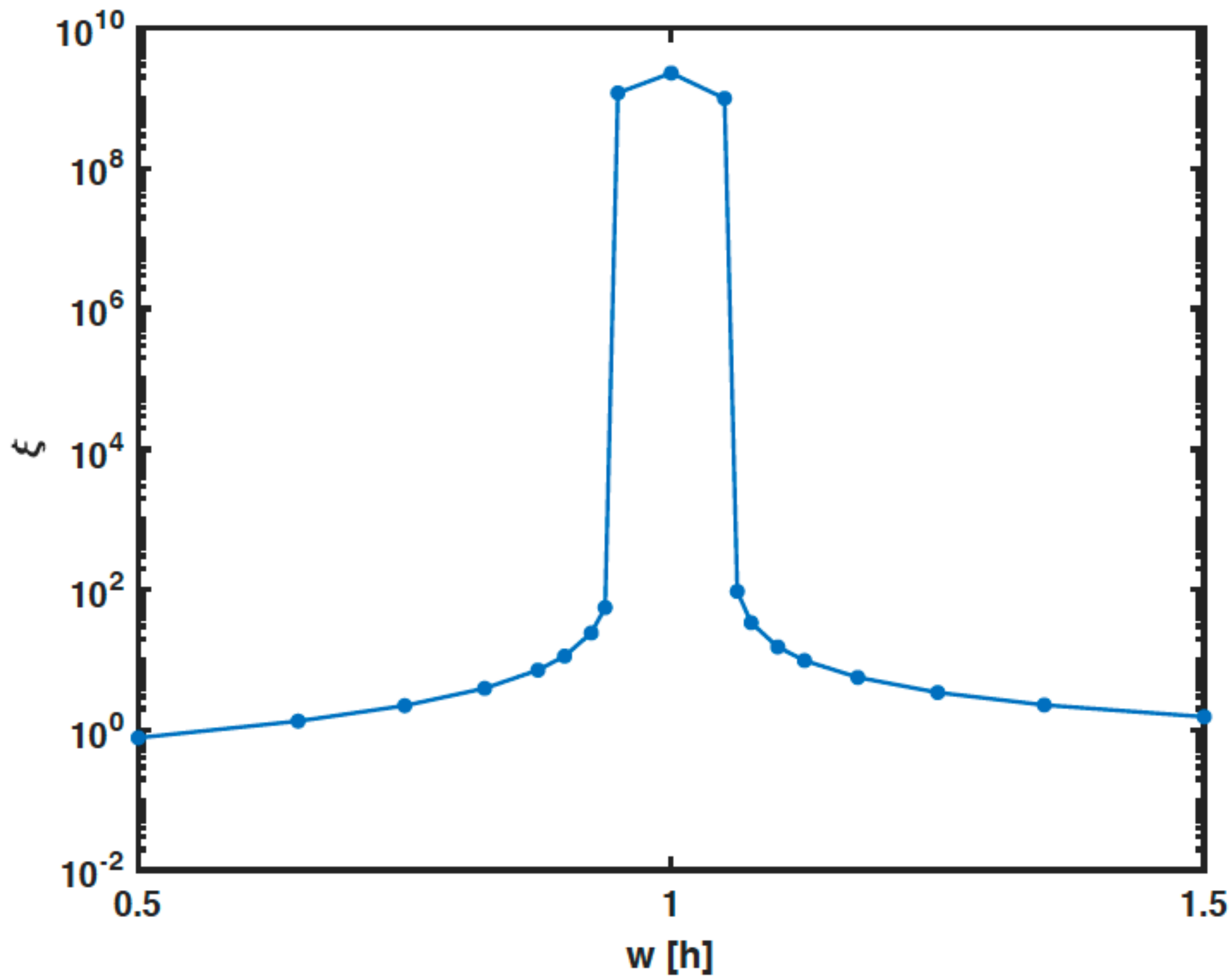

Figure 12: Correlation length ξ from fit of $C_{n,n}(j_1, j_2)/C_{n,n}(j_1, j_1)$, as a function of w. Note the divergence at the phase transition point $w = 1$. Note that the correlation length is really infinite only at the transition point for an infinite system: For extracting a good estimate of the correlation length close to $w = 1$ one has to use larger and larger system sizes as $w \to 1$. The correlation length ξ is here extracted using $L = 200$, therefore its estimate close to $w = 1$ is inaccurate, and one has to do a proper finite-size scaling. This is useful if one wants to extract critical exponents associated with a phase transition. However $L = 200$ is still sufficient to observe the diverging behavior.

3. Excess population near edges due to populated edge states.

- With $n_{edge} = n_1 + n_2$, compute

$$N_{edge} = \langle \Psi_0 | n_{edge}(t) | \Psi_0 \rangle = \langle \Psi_0 | e^{iH_f t} n_{edge} e^{-iH_f t} | \Psi_0 \rangle,$$

where $H_f = H(h=1.0, w=0.5)$ is the post-quench Hamiltonian, but $|\Psi_0\rangle$ is composed of $|\varphi_1\rangle, \ldots |\varphi_{L+1}\rangle$ of initial Hamiltonian $H_i = H(h=0.5, w=2.0)$.

- Time-evolution only relies on $u(t) = e^{-ih_f t}$ (see A.3), to compute $|\varphi_1(t)\rangle = u(t)|\varphi_1\rangle, \ldots, |\varphi_{L+1}(t)\rangle = u(t)|\varphi_{L+1}\rangle$

$\rightsquigarrow$ Compute $\langle \Psi(t) | n_{edge} | \Psi(t) \rangle$ analogous to problem 2.

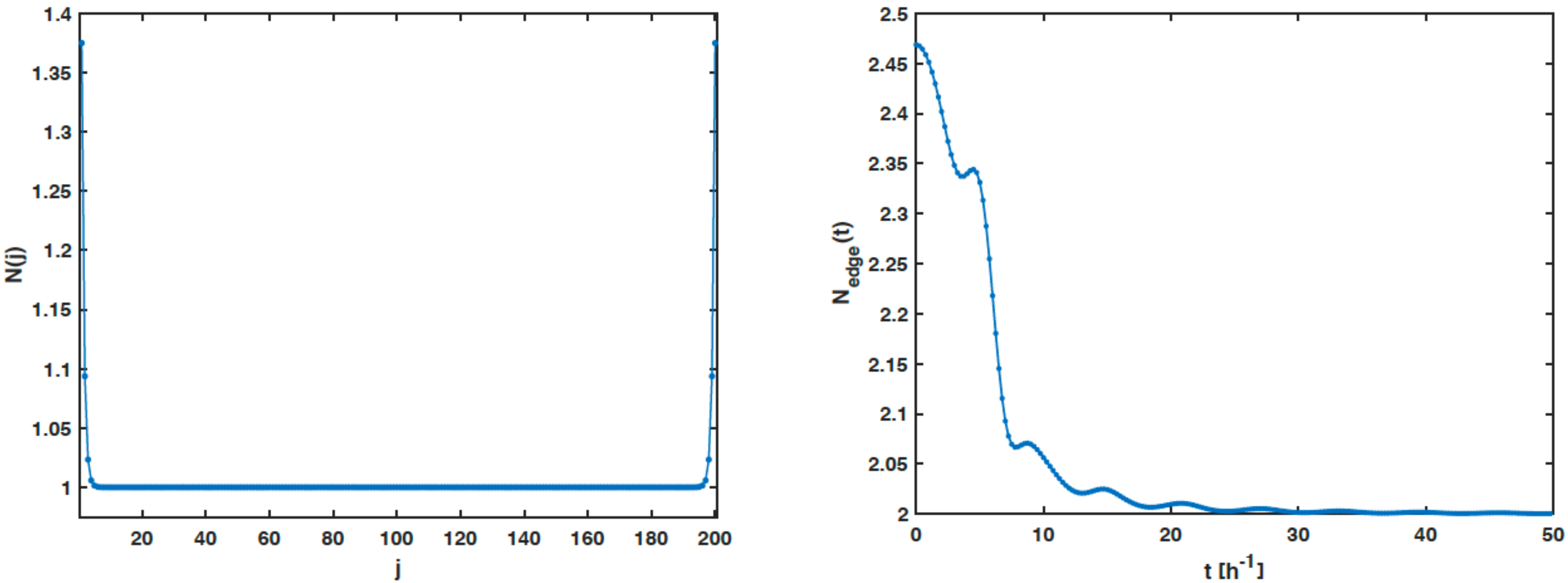

Figure 13: Left panel: Density profile $N(j)$ for $h = 1$, $w = 2.0$ with $L = 200$ and $N_{part} = 201$. Right panel: Post-quench time-evolution of the edge population $N_{edge}(t)$.

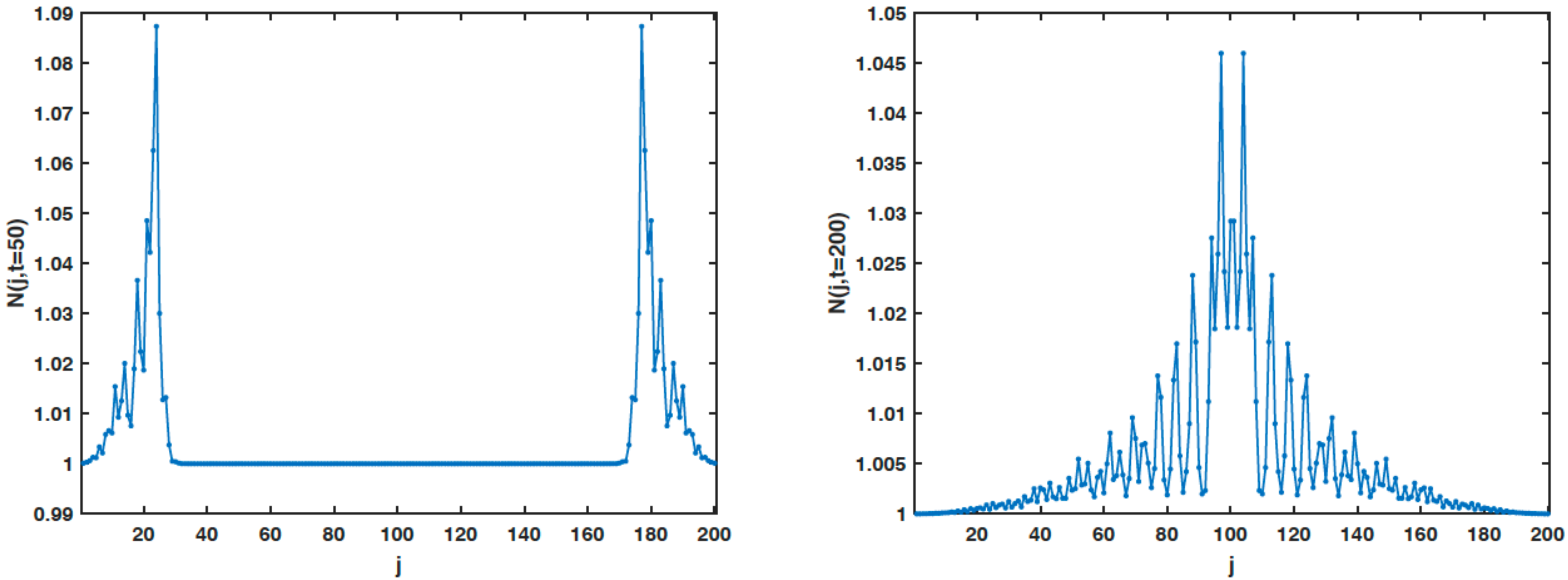

Figure 14: Left panel: Post-quench density profile $N(j)$ at $t = 50\,h^{-1}$. The pre-quench end-states, occupied at $t = 0$, behave like wave-packets that propagate in the bulk from the chain. Right panel: Post-quench density profile $N(j)$ at $t = 200\,h^{-1}$, when the two wave-packets meet.

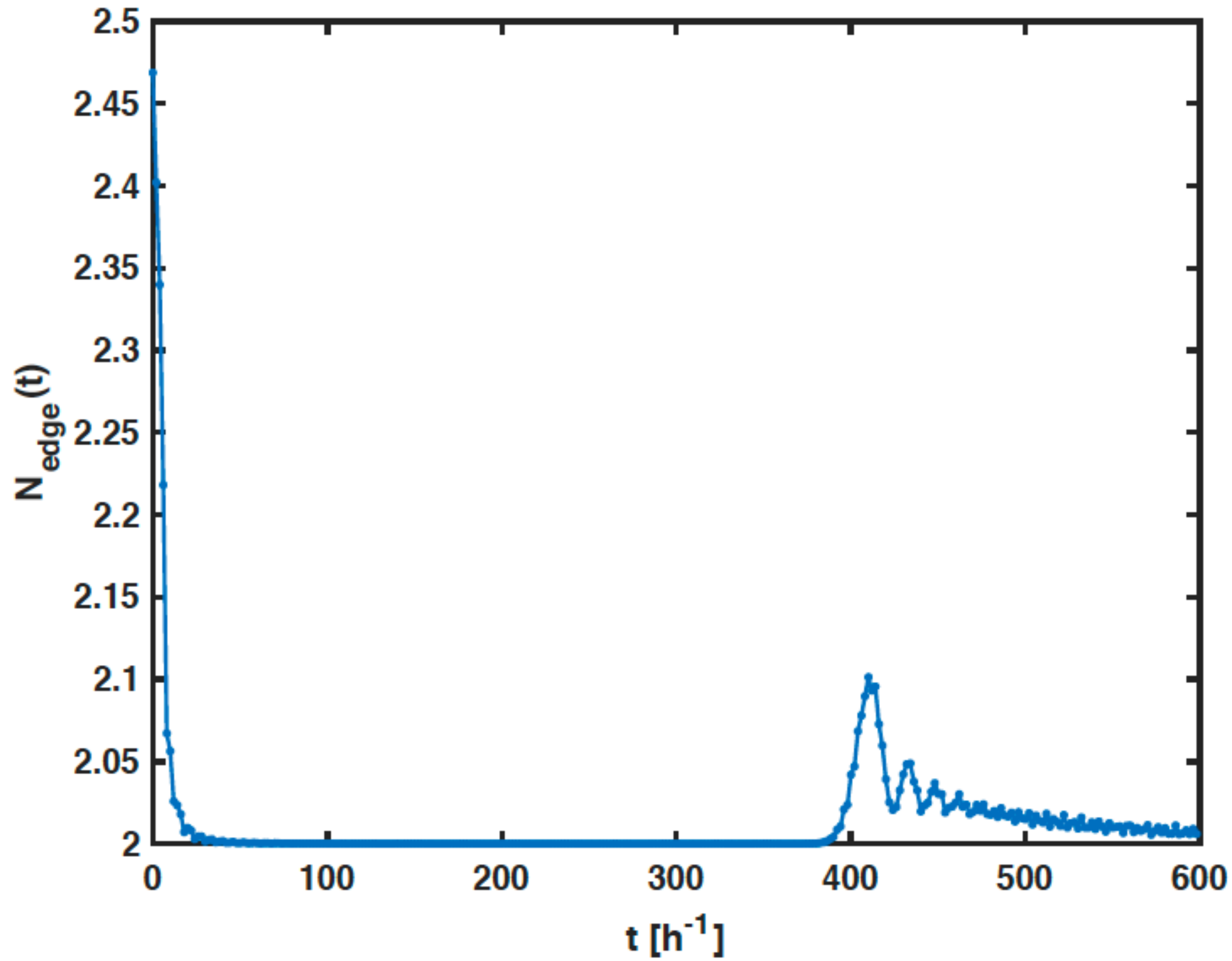

Figure 15: Post-quench time-evolution of the edge population $N_{edge}(t)$ at long times, showing the revival when the wave-packet initialized at one end reaches the opposite end and is reflected.